Evaluating the mixing performance in a planar passive micromixer with t-shape and SAR mixing chambers: comparative study

Ababneh, Jafar; Deif, Mohanad A.; Solyman, Ahmad; Zekry, Rahma S.; Hafez, Mohamed; Sharfo, Samer M.

Published in:
2023 2nd International Engineering Conference on Electrical, Energy, and Artificial Intelligence (EICEEAI)

DOI:
10.1109/EICEEAI60672.2023.10590004

Publication date:
2024

Document Version
Author accepted manuscript

Evaluating The Mixing Performance in A Planar Passive Micromixer With T-shape and SAR Mixing Chambers: Comparative Study

Jafar Ababneh
The Faculty of Information Technology, *Cyber security,*
Zarqa University, Zarqa, Jordan
College of Engineering
University of Business and Technology
Jeddah, Saudi Arabia
jababneh@zu.edu.jo

Mohanad A. Deif
Department of Artificial intelligence ,
College of Information Technology,
Misr University for Science & Technology (MUST)
6th of October City 12566 , Egypt
Mohanad.Deif@must.edu.eg

Ahmad Solyman
School of Computing, Engineering and Built Environment, Glasgow
Caledonian University
Glasgow, UK
ahmed.solyman@gcu.ac.uk

Rahma S. Zekry
Department of Bioelectronics, Modern University of Technology and Information (MTI) University
Cairo, Egypt
RAHMA.91138@eng.mti.edu.eg

Mohamed Hafez
Faculty of Engineering FEQS
INTI-IU-University
Nilai, Malaysia
mohdahmed.hafez@newinti.edu.my

Samer M. Sharfo
Department of Bioelectronics, Modern University of Technology and Information (MTI) University,
Cairo, Egypt
samer.86027@eng.mti.edu.eg

***Abstract*—In Microfluidic devices have gained significant interest in various fields, including biomedical diagnostics, environmental preservation, animal epidemic avoidance, and food safety regulation. Micromixing phenomena are crucial for these devices' functionality, as they accurately and efficiently manipulate fluids within microchannels. The process aims to blend samples accurately and swiftly within these scaled-down devices, governed by the promotion of dispersion among distinct fluid species or particles. Advancements in passive and active micromixers have led to innovative designs incorporating diverse processes to enhance mixing efficiency. Examples include two-dimensional impediments, controlled imbalanced collisions, and complex configurations like spiral and convergence-divergence structures. Active micromixers use external cues to initiate and regulate mixing processes, including thermal, magnetic, sound, pressure, and electrical fields. The trajectory of micromixing technologies is significantly influenced by current developments in microfluidics. One notable advancement is the incorporation of micromixers into 3D printing methodologies, facilitating the development of adaptable microfluidic systems. Additionally, the incorporation of microfluidic principles into paper-based channels creates opportunities for the development of cost-effective and portable diagnostic devices. The process of micro-mixing is critical in boosting the functionalities of these devices.**

Keywords*—*T-shape channels, SAR channels, Computational fluid dynamics (CFD), Pressure drop, 3D printing integration, Fluid dynamics, Micromixer, Passive Micromixer, Active Micromixer, Microfluidics, Lab on a Chip (LoC).

I. INTRODUCTION

Microfluidics has evolved into a crucial instrument across a spectrum of domains, spanning from the life sciences [1] to applications in environmental and chemistry analysis[2]. In chemical engineering, microfluidics plays a pivotal role in improving critical factors like space-time yields, selectivity, residence times of reactions, and the efficiency of conversions during fundamental synthesis processes conducted in solution[3].

Lab-on-a-chip (LOC) instruments offer a comprehensive and standardized framework for conducting various procedures and diagnostics on tiny samples[4]. Microfluidic technology, namely Lab-on-a-Chip (LOC) instruments, is extensively utilized in chemical, medical engineering, and biological domains. Microfluidic mixers play a crucial role in these devices by enabling the homogenization of several fluid streams. It is worth noting that the predominant approach to the operation and design of microfluidic mixers is centered on laminar flow patterns[5].

To provide an illustration example, a contemporary task involves achieving harmonious blending between immiscible fluids and producing precisely calibrated droplets. In addition, these microfluidic platforms provide a wide range of functionalities, such as the precise manipulation of crystallization or polymerization processes for complex molecules. Various techniques are employed in diagnostics, including absorption spectrometry, pH measurement, and the quantification of biological cells. These techniques play crucial roles in biomedical analyses[6].

Numerous researchers are advancing microfluidic systems that integrate innovative optical diagnostics to enumerate and assess morphology, size, and particle concentration, offering a more comprehensive characterization[6]. The minute dimensions of flow channels within microfluidic systems increase the surface-to-volume ratio, rendering them advantageous for many applications[7]. Nevertheless, achieving adequate micromixing at low Reynolds numbers primarily relies on molecular diffusion, necessitating a transition where convection predominates over diffusion through active or passive means[8].

For the enhancement of mixing efficiency, active micromixers necessitate the utilization of external energy sources[9],[10]. Conversely, passive micromixers predominate over their active counterparts due to their more straightforward construction and reduced manufacturing and operational expenses. As a result, microfluidic mixing approaches can be divided into two main categories: "active,"

which involves applying external energy to disturb the sample components, and "passive," where specifically engineered microchannel designs enhance the contact area and duration of interaction among the sample components[11].

The primary aim of passive micromixers is to enhance mixing efficiency by facilitating diffusive mixing by augmentation of contact area and contact time among multiple species[7]. These passive micromixers are characterized by intricate channel geometries, with many studies focusing on various passive micromixer types [12]. Standard designs include serpentine [13]and convergent-divergent [14] microchannels. Chen et al. conducted simulations and analyses involving a serpentine microchannel with six distinct shapes[15].

Furthermore, investigations have been conducted involving numerical and experimental analyses of convergent-divergent micromixers[16]. Usefian and Bayareh introduced a practical design for a convergent-divergent micromixer[17]. Passive micromixer efficiency can be augmented through two fundamental mechanisms: the generation of transverse flow motion to induce chaotic advection and the enhancement of lamination via molecular diffusion. To amplify the interfacial area, lamination-based channels such as Y-type and T-type mixers merge two divided flows[18]. Given that advection-based mixers enhance mixing performance by creating secondary flows perpendicular to the primary flow stream, they are more widely employed[8].

Afzal and Kim introduced a micromixer design that incorporates a sinusoidal modification of its geometric profile[19]. In another research project, they explored the combined impacts of pulsatile flow and convergent-divergent geometry[20]. Furthermore, an in-depth quantitative analysis of the geometric parameters of zigzag, square-wave, and curved microchannels was conducted by Hossein et al.[21]. Their research revealed that the curved mixer boasts the lowest pressure drop while the square-wave mixer attains maximum mixing efficiency. A separate study [22]assessed the mixing efficiency of square-wave, multi-wave, and zigzag microchannels across a broad range of Reynolds numbers. Their findings demonstrated that the square-wave Micromixer outperforms the other two types, albeit with a higher pressure drop associated with mixing.[23] conducted a comprehensive study encompassing simulation, fabrication, and assessment of a micromixer. In their initial phase, simulation was employed to determine the required length or volume to ensure adequate mixing. This entailed the resolution of the Navier–Stokes and continuity equations, alongside the mass conservation equation for the enzyme, employing the commercial software COMSOL.

In the fabrication process of the Micromixer, an imide-based photo-imageable dry film served as the substrate material, which was then laminated onto a Printed Circuit Board (PCB). The film demonstrated exceptional characteristics, such as biocompatibility and improved chemical and thermal stability, compared to other polymers. Significantly, the material's photosensitivity facilitated a favorable fabrication technique for cost-effective mass production. Furthermore, this film facilitated the smooth incorporation of the Micromixer into many other microfluidic components within complex Lab-on-a-Chip (LoC) platforms. It is essential to acknowledge that polyimide has been utilized as a substrate material in polymerase chain reaction (PCR) devices[24]. However, it is worth mentioning that the microfluidic chambers or channels in these devices have traditionally been created by laser ablation or plasma etching methods, which have not yet been implemented for the large-scale manufacture of microfluidic systems.

The artificially created Micromixer was assessed regarding its effectiveness in DNA digestion. A segment of a Polymerase Chain Reaction (PCR) sample, comprising an amplified product of 273 base pairs (bp), was combined and subjected to a reaction with a restriction enzyme at a temperature of 37 °C without the need for supplementary incubation stages[25]. Notably, this procedure successfully achieved complete digestion at a timeframe comparable to the traditional technique's incubation period. It is worth mentioning that literature regarding the utilization of micromixers for on-chip enzymatic digestion[26] is scarce.

In contrast to previous studies where enzymatic digestions were conducted either in a batch mode using static microreactors or continuous flow digestion microdevices, this research introduces the creation of a continuous flow passive Micromixer. This Micromixer serves a dual role by efficiently blending DNA with the enzyme and facilitating digestion. Beyond its intended application, the significance of this work lies in the fabrication technology applied to the Micromixer, enabling the integration of microfluidic devices with various components such as electronic circuits, sensors, and microheaters. These integrated components have the potential to play a crucial role in on-chip detection and control, providing a cost-effective approach in line with the current trends in Lab-on-a-Chip (LoC) technology[27].

A. Micro-fluidic Applications

The utilization of cell-free DNA (cfDNA) has become a vital element in precision oncology, garnering considerable interest for its exceptional ability to provide insights into important facets of cancer, such as genomic alterations, tumor load, and drug resistance. Among its numerous applications, determining cfDNA concentration has become a robust and independent prognostic biomarker directly linked to cancer patients' overall survival. Nevertheless, the intrinsic characteristics of cell-free DNA (cfDNA), marked by limited quantity and considerable fragmentation, provide significant obstacles to insolating and subsequently analyzing these crucial molecules[28].

In the present scenario, microfluidic technologies and lab-on-a-chip (LOC) instruments have emerged as revolutionary instruments that provide potential solutions to these difficulties on a microscale level. By functioning at the micrometer scale, these technologies effectively decrease the necessary sample volume, enabling the practical implementation of rapid and efficient separation of cell-free DNA (cfDNA). In addition, microfluidic devices offer significant automation, allowing for efficient and streamlined high-throughput screening processes without the requirement for laborious liquid transfers. This implies that the efficient and accurate analysis and measurement of cfDNA can be smoothly incorporated into a unified and efficient process[29].

The ramifications of these achievements are significant. Lab-on-a-chip (LOC) instruments and Microfluidic technologies not only enhance the efficiency and effectiveness

of working with cell-free DNA (cfDNA) for researchers and physicians, but they also facilitate speedy, precise, and high-throughput analysis[30]. This study contributes to our comprehension of cancer at the molecular level and can potentially significantly transform diagnostics, treatment monitoring, and therapeutic decision-making in precision oncology[31].

current difficulties

One of the significant challenges faced in the present era pertains to collecting real-time, high-performance quantitative data related to operations at the micrometer scale[32]. Although lab-on-a-chip (LoC) configurations hold immense potential, a substantial portion still rely on bulky, expensive benchtop devices to characterize analytes and products. This dependence on larger equipment diminishes their appeal compared to techniques and traditional protocols, especially in real-world applications beyond controlled laboratory settings[33]. To address this, various detection and characterization systems leveraging electrochemical, magnetic, or optical transducers have been integrated with LoC devices, striving to create more compact analytical platforms[3].

When employing diverse configurations, such as curved channels [34],[35],[36] and convergence-divergence designs[37],[20], within micromixers, numerous challenges may arise, including issues within the microchannel itself [38] or on its walls [39]. Different obstacles have been proposed to optimize mixing efficiency within shorter channel lengths encompassing chevron patterns, arcs, leakage side channels, triangles, and grooves [8]. Remarkably, despite their effectiveness in characterizing continuous phases or effective media [40],[33],[41], the development of tools for characterizing disperses phases (e.g., droplets, bubbles, crystals, or aggregates) remains in its nascent stages[3].

The acoustofluidic mixer can mix highly viscous fluids.

Obtaining fluid mixing without turbulence or convection relies solely on molecular diffusion. This challenge becomes particularly pronounced when dealing with viscous fluids, a difficulty that extends to microfluidic setups, given that higher viscosities lead to lower Reynolds numbers [7],[42],[43]. It's imperative to recognize that the efficacy and sensitivity of assays are intricately linked to the performance of mixing processes[44].

In contrast to passive micromixers, active micromixers offer a smaller overall footprint and the ability to rapidly mix liquids within confined volumes, even in scenarios devoid of fluid flow. However, active micromixers necessitate external energy sources. A broad spectrum of external sources, including pressure [45],[46], acoustics[47],[48], magnetic fields[49],[15], electric fields[50],[42], and thermal fields [51],[52], has been harnessed to create diverse types of active micromixers.

B. *Types of Micro-Mixers*

1. Active micromixers

Active micromixers are a category of microfluidic devices that employ external energy sources to disturb fluid flow, resulting in enhanced interaction between various fluid components and the induction of turbulent advection. The methods above contribute to enhancing the mixing effect within the microfluidic system. The classification of active micromixers is determined by the particular sorts of external energy sources utilized, each contributing to different approaches for adequate mixing.

i. Pressure Field Driven Micromixers

Typically, pressure field-driven micromixers exhibit straightforward layouts, commonly consisting of a primary channel coupled with one or more side channels or the intersection of two cross channels[53].

The fundamental concept underpinning conventional pressure field-driven micromixers revolves around an alternating perturbation approach, initially introduced by Deshmukh et al. in 2000. This approach employs pulsatile flow micropumps to provide alternating disturbances to the flowing fluids. Subsequently, similar micromixers employing this principle have been developed for merging two fluids characterized by distinct flow properties and hydrodynamic behaviors [54]. A commonly seen arrangement of a pulsatile pressure-driven micromixer is the incorporation of two micropumps in combination with a conventional T-type channel [55]. The micropumps inject the two fluids consecutively into the channel, thereby substantially increasing the contact area between them. This heightened interaction enhances the diffusion process and elevates the overall mixing efficiency.

ii. Electrical Field Driven Micromixers

The fundamental principle of electrical field-driven micromixers is based on electro-hydrodynamic (EHD) instability. This phenomenon typically involves the motion of electrically charged fluids under the influence of alternating current (AC) or direct current (DC) electric fields to disrupt the fluid interface. Notably, the significance of interfacial charge at solid-liquid boundaries distinguishes electro-kinetics (EKI), a subfield within electro-hydrodynamics (EHD). EKI elucidates the intricate relationship among ion transport, fluid dynamics, and electric fields.

Under the influence of strong electric fields and a gradient in electrical conductivity, electrokinetic flow instabilities become apparent. Electrokinetic (EKI) comprises two primary configurations. Type I features an arrangement where the electric field and the conductivity gradient are perpendicular to each other. In contrast, Type II involves a non-trivial distribution of net charge density, even in the base state, with the electric field aligning parallel to the conductivity gradient.

iii. Sound Field Driven Micromixers

Sound field-driven micromixers operate on the principle of acoustic resonant disturbance, utilizing a Lamb-wave membrane device to enhance the mixing process. These micromixers often rely on microbubbles to achieve swift convective mixing. Initially, Hashmi et al. introduced a micromixer based on bubbles in the acoustic field, incorporating a microstreaming flow field. This innovation notably enhanced DNA hybridization rates, increasing them by around five times [56]. However, this approach generated excessive bubbles within the channel[57].

Subsequently, Ahmed et al. devised a novel approach by entrapping air bubbles within a "horse-shoe" structure, generating microstreaming effects within the microchannel. This innovation led to the development a single-bubble-based acoustic micromixer, demonstrating the capability to achieve complete mixing in a mere 7 milliseconds.

In an alternative approach, another prevalent sound field-driven micromixer utilizes a surface acoustic wave (SAW) that travels along the surface of a solid substrate. This SAW is generated by interdigitated electrodes deposited on a piezoelectric substrate, inducing disturbances and turbulence in the transverse acoustic streaming, consequently enhancing mixing through the transferred sound energy [58].

iv. Magnetic Field Driven Micromixers

Magnetic field-driven micromixers' foundational principles are magneto-hydrodynamics (MHD) and magnetic stirring. These micromixers harness Lorentz forces acting upon magnetically responsive fluids by applying magnetic fields, which can be AC and DC electric fields. The resultant magneto-hydrodynamic micromixers generate secondary flows within the fluid, serving the dual purpose of stirring and mixing.

One exemplar of a magneto-hydrodynamic micromixer features double-sided sidewalls with individually controlled electrodes and an electrolyte solution. When exposed to a consistent magnetic field, this Micromixer functions as a mixer and a pump. In recent research, ferrofluids have widely been used to develop micromixers[59],[60].

For instance, Cao et al. engineered a ferrofluid-based microfluidic magnetic micromixer, employing a hybrid magnetic field generated by small micro-magnets and an external AC uniform magnetic field. This setup applies periodic magnetic forces to the ferrofluid, producing a high mixing efficiency of 97% within 8 seconds, even when the mixing channel inlet is 600 meters away.

Another approach implemented by Nouri et al. involves a ferrofluid-based magnetic mixer, which employs a Y-shaped microchannel and a permanent magnet. The permanent magnet's magnetic field prompts the ferrofluid to move from one of the bottom sides of the channel to the top side, facilitating the mixing of deionized water and Fe3O4 ferrofluid.

Additionally, magnetic stirring micromixers frequently adopt magnetic stirrers driven by externally positioned rotating magnetic fields to induce fluid mixing within the chamber.

v. Thermal Field Driven Micromixers

Thermal bubbles are pivotal in thermal field-driven micromixers, facilitating the mixing process. Huang and Tsou presented a microfluidic device driven by thermal bubbles, which was based on a silicon-on-insulation (SOI) wafer. This device incorporated a microvalve, micropump, and micromixer[52]. When the flow rate remained below 4.5 L/s, the size of thermal bubbles could be regulated. These thermal bubbles formed periodically and rapidly collapsed in response to a high-frequency AC signal supplied to the micro-heater. This dynamic behavior induced turbulent flow within the fluids, significantly enhancing mixing efficiency.

Micromixers that employ the electrothermal effect encompass a range of multiphysics phenomena that can be harnessed to achieve efficient mixing [22]. An electrothermal micromixer was introduced by Kunti et al., which utilizes alternating current and incorporates eight pairs of asymmetric electrodes that are energized by an AC voltage source. The Micromixer's floor exhibits a wavy design that enhances the contact area between the two fluids. Additionally, the top wall of the Micromixer features symmetric electrode pairs that generate lateral vortex pairs. The arrangement above demonstrated a flow velocity of 1.794 m^2/min and a notable mixing efficiency of 97.25%.

vi. Additional Micromixers Driven by External Fields

Centrifugal forces have been widely utilized in micromixers to augment the mixing process [61],[62]. The centrifugal Micromixer invented by Haeberle et al. [63] employed the Coriolis force generated by a spinning plate to facilitate fluid propulsion and mixing. Meanwhile, Leung et al. assessed mixing efficiency in various spinning radial microchannels featuring diverse obstruction patterns and width-constriction geometries, all based on the principles of centrifugal micromixing.

Experimental results demonstrated that the arrangement employing obstruction with constriction (OWC) and the influence of Coriolis and local centrifugal acceleration substantially augmented transverse flow within the microchannel. Particularly noteworthy was the rotating OWC (obstruction followed by width-constriction) channel, which achieved an impressive mixing efficiency of up to 95% when positioned 30 mm away from the inlet, with a rotation rate of 73 rad/s, surpassing the performance of stationary OWC channels, rotating unobstructed/obstructed channels, and rotating width-constricted channels**.**

2. Passive Micromixer

Static micromixers, also known as passive micromixers, harness the microchannel structure to achieve adequate mixing through a combination of chaotic advection and molecular diffusion. Recent progress in passive micromixers has been driven by scientific research. These micromixers can be categorized based on their structural dimensions, falling into two distinct categories: two-dimensional (2D) and three-dimensional (3D).

I. 2D Passive Micromixers

The ease of building and inducing chaotic advection in two-dimensional (2D) passive micromixers with flat configurations, including structures like obstacles, uneven collisions, convergence-divergence channels, and spiral channels, can be attributed to the unique characteristics of the channel layout.

II. Obstacle Based Micromixers

Many forms and heights are commonly observed in obstacle-based micromixers' embedded grooves or obstacles. The initial proposition involved a conventional obstacle-based micromixer featuring straight grooves [64]. The experimental findings indicated that within a wide range of Reynolds numbers ($0 \leq Re \leq 100$), the straight grooves utilized in the

research induced a secondary flow within the channel, leading to efficient mixing. Howell et al. [65] enhanced the design by incorporating grooves on both the upper and lower surfaces of the channel. Additionally, Hossain et al. [66] further optimized this Micromixer, and simulation results suggested that the maximum achievable mixing efficiency could reach as high as 91.7%. However, barriers within the channels remain a recurring challenge for these micromixers. In their study, Bhagat et al. (year) investigated the influence of barrier height and shape on mixing effectiveness (Bhagat et al., [67]

III. Unbalanced Collision-Based Micromixers

The performance of collision-based micromixers might be affected by an asymmetrical channel construction or fluctuations in fluid flow rates, resulting in imbalances. The advancement of a commonly encountered collision-based micromixer entailed the application of cross-collisions and imbalanced splits of fluids. The topic in question was first introduced by Ansari et al. in their publication [18]. The principal determinant of the mixing phenomena can be attributed to the synergistic interplay of Dean vortices and imbalanced collisions. Hossain et al. (year) also conducted a study that devised a micromixer comprising three asymmetrical rhombic sub-channels akin to the one expounded in this investigation. Their simulation study revealed that when the Reynolds number was set at 60, the mixing efficiency of the unbalanced three-split rhombus-based Micromixer was observed to be 86%. This value surpassed the mixing efficiency of the two-split rhombus-based Micromixer by around 1.44 times.

IV. Spiral Based Micromixers

Schönfeld et al. [68] proposed the first notion of a micromixer based on a spiral design. In their study, Sheu et al. extended the existing spiral-based Micromixer by incorporating the notion of imbalanced collisions. This resulted in the development a parallel laminar micromixer that utilizes two-dimensional staggered curved channels [69]. The curved channels facilitated the generation of Dean vortices due to centrifugal forces, while the particular configuration of the tapering channels led to an unequal partitioning of the primary fluid stream. Consequently, this design minimized the diffusion distance between the two fluids.

V. Convergence–Divergence-Based Micromixer

Micromixers featuring a convergence-divergence configuration possess the capability to generate expansion vortices. These vortices significantly disrupt the laminar flow within the microchannel and expand the contact area among different fluids. This, in turn, leads to an enhancement in mixing efficiency.

VI. 3D Passive Micromixers

To enhance the mixing process, three-dimensional (3D) passive micromixers often employ complex spatial structures. These structures can be challenging to manufacture and have the capacity to generate a range of vortices, including chaotic advection, Dean vortices, and secondary flow vortices.

VII. Lamination Based Micromixers

Micromixers based on lamination typically consist of multi-layer structures and can achieve rapid and highly efficient mixing within milliseconds. An illustrative example of such a lamination-based micromixer was initially introduced in the work of [70],[71]. They introduced a novel multi-lamination-based Micromixer with wedge-shaped vertical fluid inlets engineered for rapid and efficient mixing.

VIII. Chamber Based Micromixers

Passive micromixers frequently utilize chambers with distinctive features, like convergence-divergence configurations, recirculation systems, and counterflow arrangements, to substantially augment the effectiveness of mixing. One notable micromixer design, as described by Hai et al.[72], incorporates a chamber-based configuration, including a convergence-divergence structure resembling a trapezoid. The observed configuration results from the combined influence of stretching and folding phenomena occurring in vertical and horizontal orientations. This intricate interplay results in a notable improvement in the efficiency of fluid mixing, particularly for fluids with modest flow rates. The Micromixer was subjected to simulations, which revealed a consistently high mixing efficiency of over 80% throughout a spectrum of low Reynolds numbers ranging from 0.5 to 60. The total mixing length of the Micromixer was determined to be 3870 m.

Subsequently, a more advanced micromixer design was produced, which had chambers with shifting trapezoidal shapes. This enhanced Micromixer boasted a total mixing length of 5000 meters. The improvement was accomplished by integrating the first Micromixer with the principles of imbalanced fluid splits and cross-collisions [72].

IX. 3D Spiral Based Micromixers

The author detailed a conventional three-dimensional (3D) micromixer featuring a spiral design comprising two spiral microchannels and an upright channel [73]. This Micromixer demonstrated a remarkable maximum mixing efficiency of up to 90% when operating at Reynolds numbers (Re) exceeding 40. The presence of the upright channel played a pivotal role in facilitating the mixing process.

X. Overbridge Based Micromixers

The principle of splitting and recombination forms the fundamental concept behind overbridge-based micromixers, which typically feature three-dimensional (3D) structures interconnected by bridge-shaped channels. Li et al. (year) presented a micromixer design that utilizes an overbridge structure and incorporates splitting channels with various widths. Simulation results validated the effectiveness of this design. The Micromixer exhibited a notable mixing efficiency, exceeding 90%, across a Reynolds number (Re) range of 0.01 to 200. Furthermore, it consistently maintained this level of mixing efficiency within the Re range of 0.01 to 50 [74].

In another instance, a different researcher designed an overbridge-based micromixer based on the renowned Tesla structures [75]. This Micromixer efficiently promoted the binding interactions between antibodies and antigens, serving the purpose of cancer cell detection. It achieved an impressive mixing efficiency of 94% within a Reynolds number (Re) range from 0.1 to 100 by stacking Tesla structures on top of each other. According to simulation data, the augmentation of

the contact area between two Tesla structures was vital in enhancing the overall mixing performance.

II. METHODS

I. *Micromixer models design*

The SAR (split-and-recombination) and conventional T-shaped Micromixers are different planar passive micromixers. The dimensions of both the SAR and the T-shaped are determined to be of a total length of 6 mm and 5 mm, the width and depth of the channels are 0.133 mm and 0.2 mm, and with hydraulic diameter (Dh) of both inlets and outlets of 0.133 mm and 0.2 mm, respectively.

TABLE 1: COMPARISON BETWEEN THE SAR (SPLIT-AND-RECOMBINATION) MICROMIXER AND THE CONVENTIONAL T-SHAPED MICROMIXER

Feature	**SAR Micromixer**	**T-Shaped Micromixer**
Length	6 mm	5 mm
Width	0.133 mm	0.2 mm
Depth	0.133 mm	0.2 mm
Hydraulic diameter	0.133 mm	0.2 mm
Mixing performance	Better	Worse
Design	More complex	Simpler

Both micromixers were intended for water and ethanol, with fluid properties based on 20 ◦C water. The assessment of mixing performance for each Micromixer was conducted over a range of Reynolds numbers spanning from 0.5 to 100, whereby the Reynolds number is defined as:

$$Re = \frac{\rho U Dh}{\mu} \qquad (1)$$

Here, U signifies the fluid velocity within the inlet channel, ρ represents the fluid density, Dh denotes the inlet channel hydraulic diameter, and μ represents the fluid's dynamic viscosity.

The fluid properties of water and ethanol, namely their densities, viscosities, and diffusion coefficients, are essential considerations in the design and operation of planar passive micromixers. The fluids' densities affect the Micromixer's flow dynamics, while the viscosities affect the resistance to flow. The diffusion coefficient of the mixture affects the rate at which the fluids mix.

The densities of water and ethanol are 998 and 789 kg/m3, respectively. The viscosities of water and ethanol are 0.9×10^{-3} and 1.2×10^{-2} Pa s, respectively. The diffusion coefficient of the water-ethanol(ethanol) mixture is 1.2×10^{-9}m2 /s.

The density of water is 998 kg/m³, while ethanol's is 789 kg/m³. Water has a value of 0.9 x 10^{-3} Pa s, while ethanol has a viscosity of 1.2 x 10^{-2} Pa s. The diffusion coefficient for the water-ethanol mixture is 1.2 x 10^{-9} m²/s.

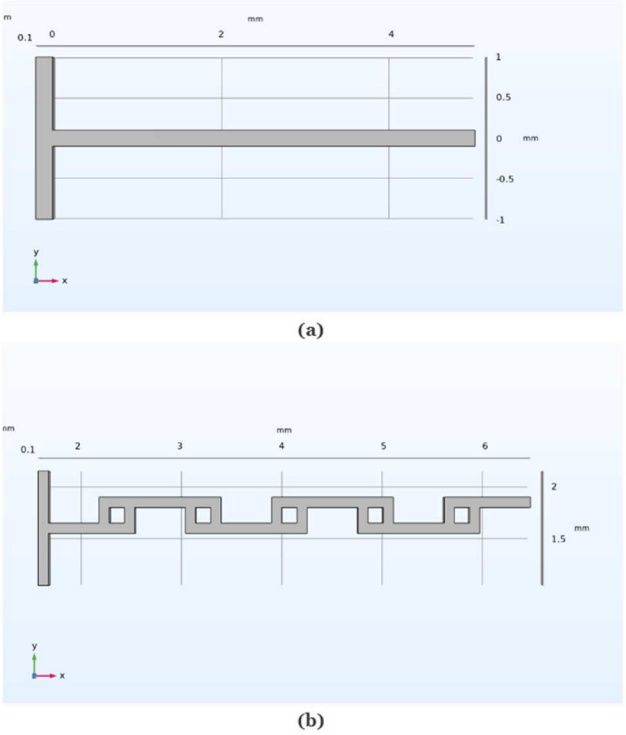

Fig.1 Schematics of the micromixer models with dimensions. (a) Conventional T-shaped Micromixer, and (b) T-advanced SAR (split-and-recombination) Micromixer.

The study's results suggest that the SAR micromixer had a higher level of mixing efficiency when compared to the T-shaped Micromixer. The SAR micromixer exhibited enhanced mixing efficiency over the range of Reynolds values. The discrepancy in mixing efficiency became more apparent when operating at higher Reynolds numbers.

The SAR micromixer's excellent mixing capability can be ascribed to its distinctive design. In contrast to the T-shape micromixer, the SAR micromixer integrates a serpentine channel that facilitates the generation of numerous vortices. These vortices are of significant importance in disrupting fluid streams and facilitating a more optimal mixing of the fluids.

In conclusion, the SAR micromixer is a viable choice for efficient fluid mixing within a planar passive micromixer. The design of the Micromixer exhibits superior performance in terms of mixing efficiency compared to the T-shaped Micromixer while also featuring a more compact and streamlined construction.

The enhanced efficacy of the SAR micromixer, in contrast to the standard T-shaped Micromixer, can be ascribed to certain crucial factors:

1) The hydraulic diameter of the SAR micromixer is less than that of the T-shaped Micromixer. As a result, the SAR micromixer demonstrates a more significant Reynolds number when operating at the same flow rate. A more significant Reynolds number indicates a flow regime characterized by increased turbulence, which promotes improved mixing.

2) The SAR micromixer exhibits a greater overall length than the T-shaped Micromixer. The increased length of the SAR micromixer allows for a longer duration during which the fluids can effectively mix and interact.

3) The SAR micromixer employs a serpentine channel architecture, whereas the T-shaped Micromixer utilizes a straight channel layout. Incorporating a serpentine channel into the fluid flow introduces more vortices, hence augmenting the mixing efficiency within the Micromixer.

II. Numerical simulation

The study utilized the computational fluid dynamics (CFD) software COMSOL Multiphysics 6.0 to solve the governing equations associated with fluid flow and mixing in planar passive micromixers, including Conventional T-shaped and SAR Micromixers. The governing equations comprise the comprehensive representation of the Navier-Stokes, continuity, and species diffusion-convection equations. They can be stated in the following manner:

$$\rho\left[\frac{\partial \mathrm{u}}{\partial \mathrm{t}} + (u.\nabla)\mathrm{u}\right] = -\nabla \mathrm{p} + \mathrm{u}\nabla^2 u \qquad (2)$$

$$\nabla \mathrm{u} = 0 \qquad (3)$$

$$\frac{\partial \mathrm{c}}{\partial \mathrm{t}} = \mathrm{D}\nabla^2 \mathrm{c} - \mathrm{u}\,.\nabla \mathrm{c} \qquad (4)$$

Number footnotes separately in superscripts. Place the actual footnote at the bottom of the column in which it was cited. Do not put footnotes in the abstract or reference list. Use letters for table footnotes.

where, "u" represents the velocity of the fluid, "ρ" denotes the density of the fluid, "p" signifies the pressure of the fluid, "μ" corresponds to the dynamic viscosity of the fluid, "c" represents the concentration of the species constant and "D" indicates the coefficient of the species diffusion.

Since this study pertains to a stationary condition that does not vary with time, both ∂c/∂t and ∂u/∂t are equal to zero (0).

The mixing efficiency was evaluated in both SAR and T-shape micromixers through Multiphysics simulations employing COMSOL Multiphysics 6.0. Both micromixers were subjected to modeling in a 3D fluid environment, with identical Reynolds number ranges (ranging from 0.5 to 100) and consistent boundary conditions. The specified boundary conditions encompassed uniform velocity profiles, equivalent volume flow rates at the inlets, zero static pressure at the outlets, an initial molar concentration of 1 mol/m3 at one inlet, a molar concentration of 0 mol/m3 at the other inlet, and the application of no-slip conditions to the channel walls. Moreover, the impact of gravity and its consequences were overlooked. To assess and quantify the extent of mixing, the species' mixing index at any given cross-sectional area within the mixing channel was computed using the following equations:

$$\sigma^2 = \frac{1}{\mathrm{N}}\sum_{i=1}^{n}(Ci - Cm)^2 \qquad (5)$$

$$MI = 1 - \sqrt{\frac{\sigma^2}{\sigma^2 max}} \qquad (6)$$

where, σ represents the molar concentration standard deviation, N signifies the total count of sampling points within the specified cross-sectional area, Ci denotes the molar concentration at the individual sampling point (i), Cm corresponds to the ideal molar concentration of a thoroughly mixed fluid, which equals 0.5 and σ_max stands for the highest standard deviation of molar concentration. The mixing index (MI) serves as a dimensionless metric, spanning from 0 (indicating 0% mixing or no mixing) to 1 (representing 100% mixing or complete mixing).

III. Results and Discussion

A. Simulation Result(velocity magnitude)

The simulation results demonstrate the velocity profile in the x-y plane for the SAR and T micromixers at various Reynolds numbers (Re = 0.5, 10, 50, 100). The data presented indicates a significant rise in velocity within the T-shaped structure, namely when the fluid stream is directed into the smaller channel. The velocity profile of the SAR micromixer demonstrates a higher level of intricacy and homogeneity than that of the T-micromixer. The increased fluid distribution observed in the SAR micromixer can be due to the employment of F-shaped mixing units, which effectively create chaotic convection. As a result, there is an improvement in the efficiency of mixing within the channels of synthetic aperture radar (SAR).

SAR Micromixer **T-shaped Micromixer**

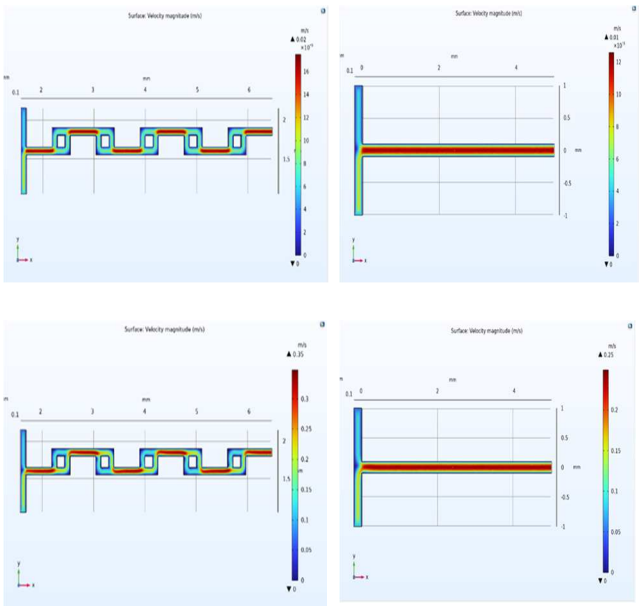

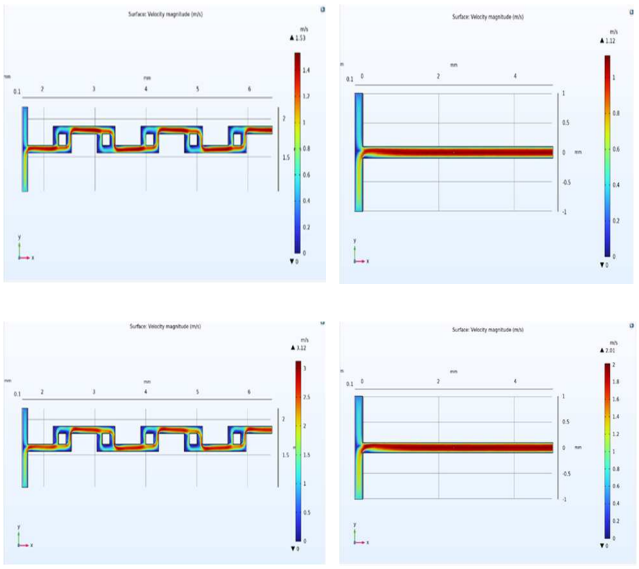

Fig.2 Comparing the Velocity magnitude for both SAR and T-Micromixers in m/s at Re = 0.5, 10, 50, and 100, respectively.

B. Simulation Result(contour pressure)

The pressure drop measures the energy required to drive the flow through the Micromixer. A lower pressure drop indicates a more efficient micromixer.

The pressure drop measures the energy required to drive the flow through the Micromixer. A lower pressure drop indicates a more efficient micromixer. MC and MI are calculated as follows:

$$MC = M * \Delta P \tag{7}$$

$$MI = 1 - \sqrt{\frac{\sigma^2}{\sigma^2 max}} \tag{8}$$

where, M is the mixing index, ΔP is the pressure drop, σ^2 represents the variance in molar concentration, and σ^2 max stands for the maximum variance in molar concentration.

The mixing index spans from 0, indicating the absence of mixing, to 1, representing the attainment of total mixing.

SAR Micromixer **T-shaped Micromixer**

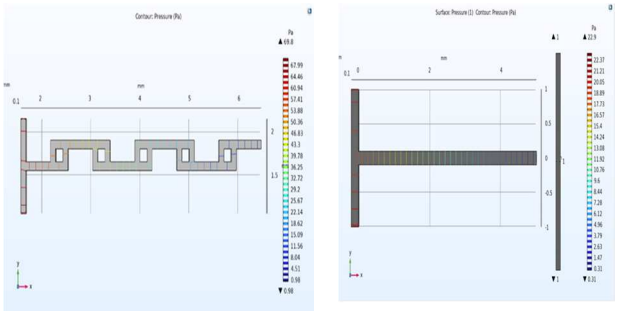

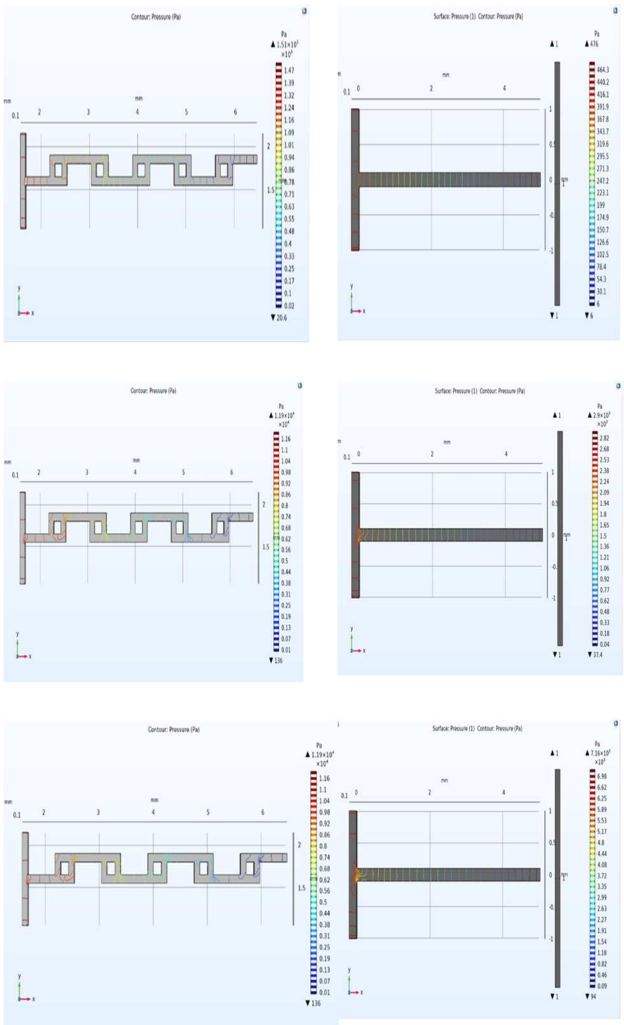

Fig.3. shows contour for both micromixers: pressure in Pa at Re=0.5, 10, 50, and 100, respectively.

Number footnotes separately in superscripts. Place the actual footnote at the bottom of the column in which it was cited. Do not put footnotes in the abstract or reference list. Use letters for table footnotes.

In summary, MC and ΔP serve as valuable metrics for assessing the mixing efficiency of planar passive micromixers, as they consider both the extent of mixing and the pressure drop.

The SAR micromixer outperforms the T-shaped Micromixer in terms of mixing efficiency. This superiority arises from using F-shaped mixing units in the SAR micromixer, which induces chaotic convection and enhances mixing. In contrast, the T-shaped Micromixer relies primarily on molecular diffusion and exhibits minimal mixing.

The analysis of the cross-sectional perspectives of the SAR micromixer provides insight into the sequential development of the mixing phenomenon. The vertical distribution of concentration gradient contours is observed within the cross-section, and despite an increase in mixing length, the presence of laminar flow patterns is still evident. In contrast, the F-shaped mixing units in the SAR micromixer

display opposing concentration gradient contours, indicating the occurrence of chaotic convection.

Conversely, the T-shaped Micromixer predominantly relies on molecular diffusion for mixing. In its cross-sectional view, the concentration gradient contours also distribute vertically, and as the mixing length increases, laminar flow patterns persist. Consequently, the mixing performance of the T-shaped Micromixer is notably inferior.

TABLE 2. SUMMARIZES THE CRITICAL DIFFERENCES BETWEEN T-SHAPED AND SAR MICROMIXERS

Micromixer	**Mixing performance**	**Mechanism**
T-shaped	Poor	Slight mixing by molecular diffusion
SAR	Better	Chaotic convection

C. Simulation Result(mixing performance)

The simulation outcomes further demonstrate that the SAR micromixer exhibits superior mixing efficiency compared to the T micromixer. In the x-y plane, the velocity distribution in the SAR micromixer is more uniform than in the T micromixer, and the pressure drop is reduced.

SAR / Advanced T- Micromixer | **Conventional T-shaped Micromixer**

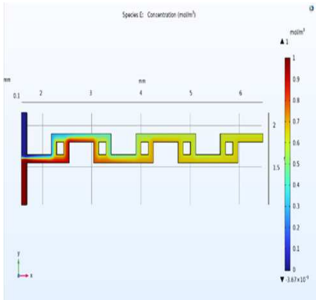
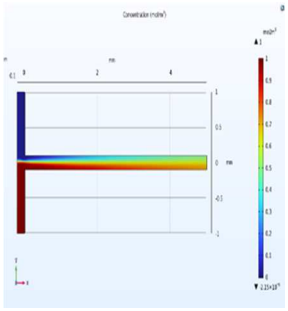

Re=0.5 | Re=0.5

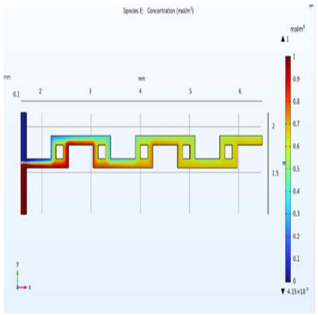
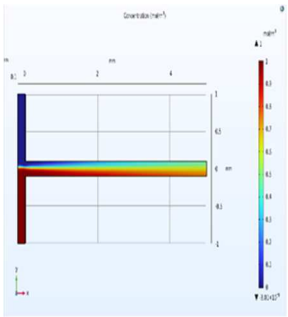

Re=1 | Re=1

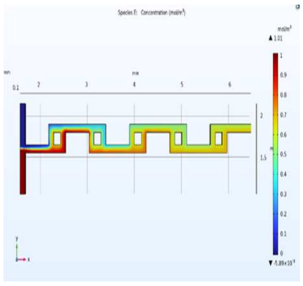
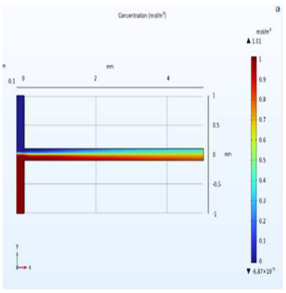

Re=5 | Re=5

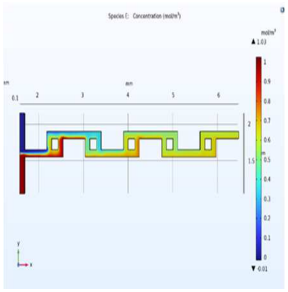
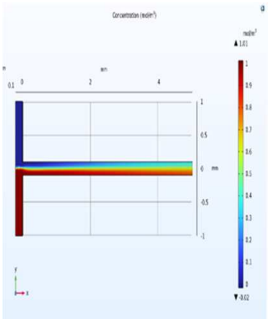

Re=10 | Re=10

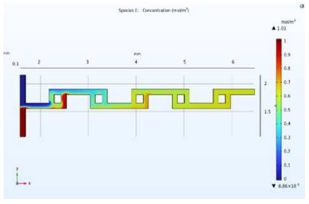
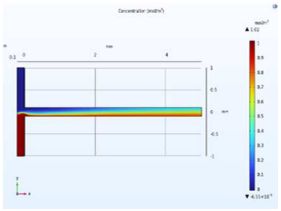

Re=20 | Re=20

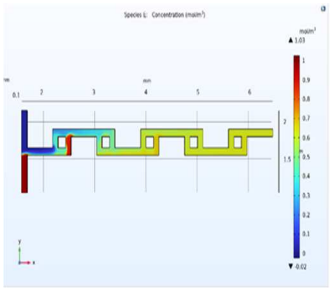
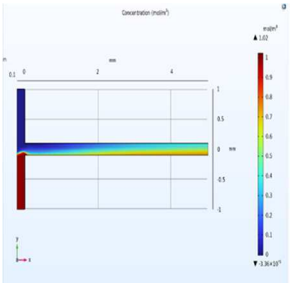

Re=30 | Re=30

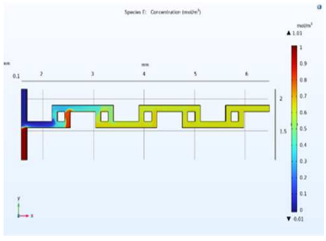
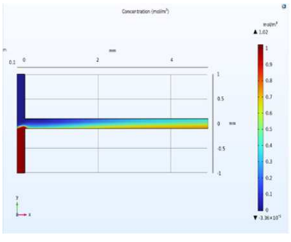

Re=50 | Re=50

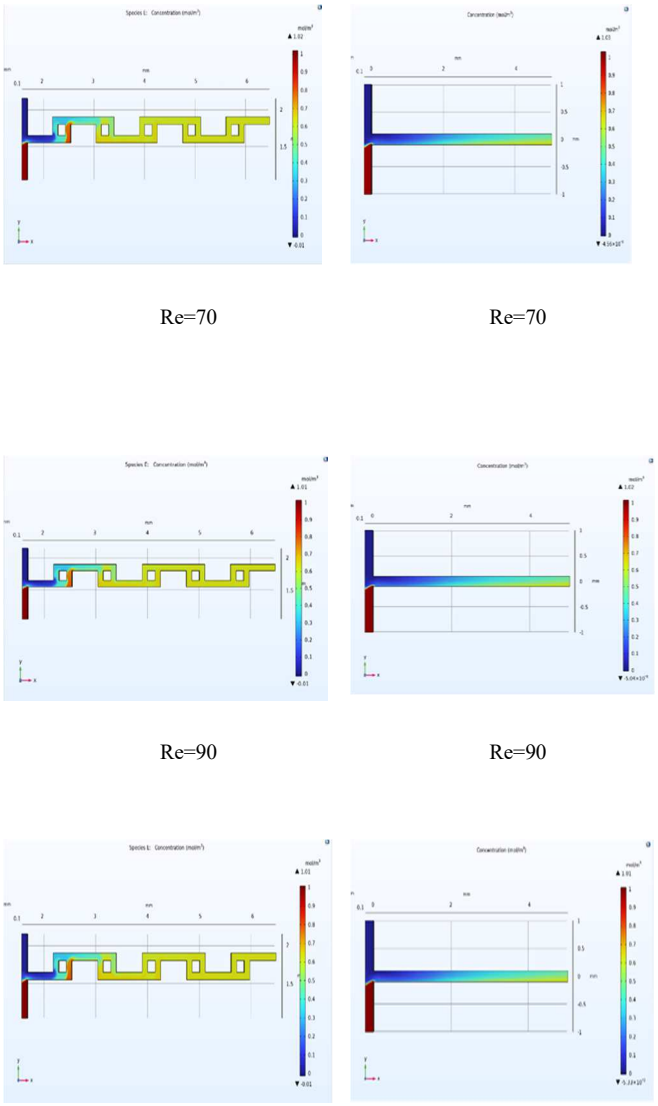

Fig.4. The assessment of mixing efficiency in SAR and T-shaped micromixers was conducted across a range of Reynolds numbers (Re = 0.5 to 100).

In summary, the SAR micromixer surpasses the T-shaped Micromixer as the superior choice for fluid mixing. It not only exhibits superior mixing performance but also operates with greater efficiency.

The SAR micromixer demonstrates a complex mixing mechanism across the entire Reynolds number (Re) range, from 0.5 to 100. Within the cross-sectional views, concentration gradient contours are predominantly distributed vertically, indicating the persistence of laminar flow patterns. However, within the cross sections of the F-shaped mixing units, a contrary pattern emerges, characterized by opposing concentration gradient contours. This phenomenon results from the fluid's traversal through two turns within each F-shaped mixing unit, generating centrifugal forces that alter the fluid ratio. This chaotic convection process significantly enhances the mixing efficiency.

The SAR, also known as the Advanced T-micromixer, consistently demonstrates superior and robust mixing performance across all Reynolds (Re) values compared to the T-shaped Micromixer. This advantage is attributed to its utilization of chaotic convection as a mixing mechanism. Chaotic convection represents a complex flow pattern within the microchannel, transitioning from orderly motion governed by simple physical laws to disorderly when encountering F-bend angles that deviate significantly from expected regularity.

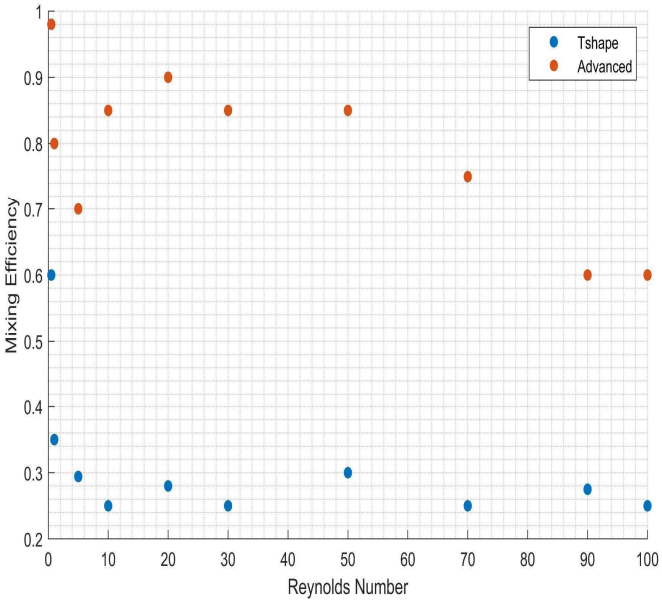

Fig.5 The change in mixing efficiency as Reynolds numbers increase at the exits of the SAR micromixer, as compared to the T-shaped Micromixer.

The SAR micromixer outperforms the T-shaped Micromixer across all Reynolds numbers (Re) ranging from 0.5 to 100.

The SAR micromixer achieves high mixing efficiency at lower Re values (<5), primarily attributed to its chaotic convection mechanism. As Re increases, mixing efficiency decreases due to reduced diffusion time. Nevertheless, at higher Re values (>5), the inertial forces generated by fluid flow contribute to improved mixing, resulting in increased efficiency.

Conversely, the T-shaped Micromixer exhibits consistently poor mixing performance across all Re values. Its mixing efficiency diminishes with rising Re due to reduced diffusion time.

TABLE 3. SUMMARIZES THE KEY FINDINGS OF THE COMPARISON BETWEEN T-SHAPED AND SAR MICROMIXERS.

SAR micromixer	• Initially, mixing efficiency is primarily influenced by molecular diffusion, a factor that diminishes as Reynolds number (Re) rises. • Once Re surpasses 5, the escalation of inertial forces disrupts the flow field, ultimately amplifying mixing. • The SAR micromixer reaches its lowest recorded mixing efficiency, 60% when the Reynolds number (Re) reaches 90 and 100.

	• In contrast, the SAR micromixer demonstrates its highest mixing efficiency of 99% at Re = 0.5. • The SAR micromixer's mixing efficiency decreases, stabilizing at 90%, as Re reaches 20.
T-shaped Micromixer	• Mixing efficiency is also initially dominated by molecular diffusion, which decreases with increasing Re. • Mixing efficiency is lowest at Re = 10, 30, 70, and 100, with values around 25%. • Mixing efficiency is slightly higher at Re = 20 and 90, with values around 28%. • Mixing efficiency is highest at Re = 0.5, with a value of 99%.

The numerical simulations evaluated the mixing performance of SAR and T-shaped micromixers across a Reynolds number range from 0.5 to 100. The SAR micromixer exhibited its highest mixing efficiency at 99% when Re was at 0.5. However, this efficiency gradually decreased to 60% as Re increased to 100. On the other hand, the T-shaped Micromixer achieved a mixing efficiency of 60% at Re = 0.5, and this efficiency dropped to 30% as Re increased to 100.

IV. Conclusion

The advancement of Micro-Electro-Mechanical Systems (MEMS) technology has resulted in notable advancements in manufacturing intricate biochips that can be applied in many fields. Micromixers have several benefits compared to larger-scale mixers, including decreased operation durations, lowered expenses, improved portability, and simplified interaction with other planar biomedical devices. The present study emphasizes the many capabilities of micromixers in a range of microfluidic applications, demonstrating their cost-effectiveness and superior performance. The primary objective of this study is to examine the mixing characteristics of T-shaped micromixers and SAR (Serpentine and Asymmetrical Radial) micromixers, employing water and ethanol as the chosen working fluids. The current investigation used COMSOL Multiphysics 6.0 software to assess the effectiveness of T-shaped micromixers in terms of their mixing efficiency across various Reynolds numbers (Re). The Reynolds numbers considered in this study include 0.5, 1, 5, 10, 20, 30, 50, 70, and 100. MATLAB software extracts graphical representations demonstrating the relationship between mixing efficiency and Reynolds number. Both micromixers employ the principles of splitting-recombination and chaotic convection mechanisms. The experimental results indicate a decline in mixing effectiveness for both T-shaped and SAR micromixers as the Reynolds number increases from 0.5 to 15. The minimum mixing efficacy of the SAR micromixer is 60% at Reynolds numbers (Re) of 90 and 100. However, it has been discovered that the mixing efficiency of the SAR micromixer demonstrates an increasing pattern throughout the Reynolds number range of 0.5 to 50, with a peak value of 98% achieved at a Reynolds number of 0.5. When the Reynolds number is above 50, a constant decrease in mixing efficiency is observed. In summary, the SAR micromixer performs better than the T-shaped Micromixer across the entire spectrum of Reynolds numbers ranging from 0.5 to 100. Furthermore, it has been observed that the SAR micromixer has a better level of mixing efficiency and demonstrates improved resistance to efficiency degradation at elevated Reynolds numbers compared to the T-shaped Micromixer.

References

[1] E. H. Sipos, A. Léty-Stefanska, C. D. Wilkes, J. Soutourina, and F. Malloggi, "Microfluidic platform for monitoring Saccharomyces cerevisiae mutation accumulation," *Lab Chip*, vol. 21, no. 12, pp. 2407–2416, 2021.

[2] J. C. Jokerst, J. M. Emory, and C. S. Henry, "Advances in microfluidics for environmental analysis," *Analyst*, vol. 137, no. 1, pp. 24–34, 2012.

[3] F. R. A. Onofri, I. Rodriguez-Ruiz, and F. Lamadie, "Microfluidic lab-on-a-chip characterization of nano-to microparticles suspensions by light extinction spectrometry," *Opt Express*, vol. 30, no. 2, pp. 2981–2990, 2022.

[4] M. Mir, A. Homs, and J. Samitier, "Integrated electrochemical DNA biosensors for lab-on-a-chip devices," *Electrophoresis*, vol. 30, no. 19, pp. 3386–3397, 2009.

[5] H. A. Stone, A. D. Stroock, and A. Ajdari, "Engineering flows in small devices: microfluidics toward a lab-on-a-chip," *Annu. Rev. Fluid Mech.*, vol. 36, pp. 381–411, 2004.

[6] A. Elsaesser *et al.*, "Future space experiment platforms for astrobiology and astrochemistry research," *NPJ Microgravity*, vol. 9, no. 1, p. 43, 2023.

[7] C. Y. Lee, C. H. Tai, C. L. Chang, C. H. Tsai, Y. N. Wang, and L. M. Fu, "Numerical simulation of electromagnetic actuator for impedance pumping," *Key Eng Mater*, vol. 483, pp. 305–310, 2011.

[8] Z. Babaie, D. Bahrami, and M. Bayareh, "Investigation of a novel serpentine micromixer based on Dean flow and separation vortices," *Meccanica*, vol. 57, no. 1, pp. 73–86, 2022.

[9] A. Usefian and M. Bayareh, "Numerical and experimental study on mixing performance of a novel electro-osmotic micro-mixer," *Meccanica*, vol. 54, pp. 1149–1162, 2019.

[10] M. Bayareh, M. N. Ashani, and A. Usefian, "Active and passive micromixers: A comprehensive review," *Chemical Engineering and Processing-Process Intensification*, vol. 147, p. 107771, 2020.

[11] C.-Y. Lee, C.-L. Chang, Y.-N. Wang, and L.-M. Fu, "Microfluidic mixing: a review," *Int J Mol Sci*, vol. 12, no. 5, pp. 3263–3287, 2011.

[12] D. Bahrami, A. A. Nadooshan, and M. Bayareh, "Numerical study on the effect of planar normal and Halbach magnet arrays on micromixing," *International Journal of Chemical Reactor Engineering*, vol. 18, no. 9, p. 20200080, 2020.

[13] N. J. Ghahfarokhi and M. Bayareh, "Numerical study of a novel spiral-type micromixer for low Reynolds number regime," *Korea-Australia Rheology Journal*, vol. 33, pp. 333–342, 2021.

[14] S. Jain and H. N. Unni, "Numerical modeling and experimental validation of passive microfluidic mixer designs for biological applications," *AIP Adv*, vol. 10, no. 10, 2020.

[15] K. Petkovic *et al.*, "Rapid detection of Hendra virus antibodies: an integrated device with nanoparticle assay and chaotic micromixing," *Lab Chip*, vol. 17, no. 1, pp. 169–177, 2017.

[16] M. K. Parsa, F. Hormozi, and D. Jafari, "Mixing enhancement in a passive micromixer with convergent–divergent sinusoidal microchannels and different ratio of amplitude to wave length," *Comput Fluids*, vol. 105, pp. 82–90, 2014.

[17] A. Usefian and M. Bayareh, "Numerical and experimental investigation of an efficient convergent–divergent micromixer," *Meccanica*, vol. 55, pp. 1025–1035, 2020.

[18] M. A. Ansari and K.-Y. Kim, "Mixing performance of unbalanced split and recombine micomixers with circular and rhombic sub-channels," *Chemical Engineering Journal*, vol. 162, no. 2, pp. 760–767, 2010.

[19] A. Afzal and K.-Y. Kim, "Mixing performance of passive micromixer with sinusoidal channel walls," *Journal of chemical engineering of Japan*, vol. 46, no. 3, pp. 230–238, 2013.

[20] A. Afzal and K.-Y. Kim, "Multiobjective optimization of a micromixer with convergent–divergent sinusoidal walls," *Chem Eng Commun*, vol. 202, no. 10, pp. 1324–1334, 2015.

[21] S. Hossain, M. A. Ansari, and K.-Y. Kim, "Evaluation of the mixing performance of three passive micromixers," *Chemical Engineering Journal*, vol. 150, no. 2–3, pp. 492–501, 2009.

[22] F. Zhang, H. Chen, B. Chen, and J. Wu, "Alternating current electrothermal micromixer with thin film resistive heaters," *Advances in Mechanical Engineering*, vol. 8, no. 5, p. 1687814016646264, 2016.

[23] V. E. Papadopoulos *et al.*, "A passive micromixer for enzymatic digestion of DNA," *Microelectron Eng*, vol. 124, pp. 42–46, 2014, doi: 10.1016/j.mee.2014.04.011.

[24] Q. I. Ahmed, H. Attar, A. Amer, M. A. Deif, and A. A. A. Solyman, "Development of a Hybrid Support Vector Machine with Grey Wolf Optimization Algorithm for Detection of the Solar Power Plants Anomalies," *Systems*, vol. 11, no. 5, p. 237, 2023.

[25] A. Alqerem, H. Attar, W. Alomoush, and M. Deif, "The Ability of Ultra Wideband to Differentiate Between Hematoma and Tumor Occur in The Brain," in *2022 International Engineering Conference on Electrical, Energy, and Artificial Intelligence (EICEEAI)*, 2022, pp. 1–7.

[26] N. Baghdadi, A. S. Maklad, A. Malki, and M. A. Deif, "Reliable sarcoidosis detection using chest x-rays with efficientnets and stain-normalization techniques," *Sensors*, vol. 22, no. 10, p. 3846, 2022.

[27] L.-M. Fu and C.-H. Lin, "A rapid DNA digestion system," *Biomed Microdevices*, vol. 9, pp. 277–286, 2007.

[28] R. E. Hammam, A. A. A. Solyman, M. H. Alsharif, P. Uthansakul, and M. A. Deif, "Design of Biodegradable Mg Alloy for Abdominal Aortic Aneurysm Repair (AAAR) Using ANFIS Regression Model," *IEEE Access*, vol. 10, pp. 28579–28589, 2022.

[29] Z. Xu, Y. Qiao, and J. Tu, "Microfluidic technologies for cfDNA isolation and analysis," *Micromachines (Basel)*, vol. 10, no. 10, p. 672, 2019.

[30] R. E. Hammam *et al.*, "Prediction of wear rates of UHMWPE bearing in hip joint prosthesis with support vector model and grey wolf optimization," *Wirel Commun Mob Comput*, vol. 2022, pp. 1–16, 2022.

[31] E. M. O. Mokhtar and M. A. Deif, "Towards a Self-sustained House: Development of an Analytical Hierarchy Process System for Evaluating the Performance of Self-sustained Houses," *ENGINEERING JOURNAL*, vol. 2, no. 2, 2023.

[32] H. U. O. Dan-Qun *et al.*, "Recent advances on optical detection methods and techniques for cell-based microfluidic systems," *Chinese Journal of Analytical Chemistry*, vol. 38, no. 9, pp. 1357–1365, 2010.

[33] I. Rodríguez-Ruiz, T. N. Ackermann, X. Muñoz-Berbel, and A. Llobera, "Photonic lab-on-a-chip: Integration of optical spectroscopy in microfluidic systems." ACS Publications, 2016.

[34] A. Alam, A. Afzal, and K.-Y. Kim, "Mixing performance of a planar micromixer with circular obstructions in a curved microchannel," *Chemical Engineering Research and Design*, vol. 92, no. 3, pp. 423–434, 2014.

[35] R. R. Gidde and P. M. Pawar, "Flow feature analysis of T-junction wavy micromixer for mixing application," *International Journal of Chemical Reactor Engineering*, vol. 17, no. 9, p. 20180306, 2019.

[36] E. Tripathi, P. K. Patowari, and S. Pati, "Numerical investigation of mixing performance in spiral micromixers based on Dean flows and chaotic advection," *Chemical Engineering and Processing-Process Intensification*, vol. 169, p. 108609, 2021.

[37] R. R. Gidde, "Concave wall-based mixing chambers and convex wall-based constriction channel micromixers," *Int J Environ Anal Chem*, vol. 101, no. 4, pp. 561–583, 2021.

[38] H. Wang, P. Iovenitti, E. Harvey, and S. Masood, "Optimizing layout of obstacles for enhanced mixing in microchannels," *Smart Mater Struct*, vol. 11, no. 5, p. 662, 2002.

[39] R.-T. Tsai and C.-Y. Wu, "An efficient micromixer based on multidirectional vortices due to baffles and channel curvature," *Biomicrofluidics*, vol. 5, no. 1, 2011.

[40] I. Rodríguez-Ruiz, M. Conejero-Muriel, T. N. Ackermann, J. A. Gavira, and A. Llobera, "A multiple path photonic lab on a chip for parallel protein concentration measurements," *Lab Chip*, vol. 15, no. 4, pp. 1133–1139, 2015.

[41] I. Rodríguez-Ruiz, F. Lamadie, and S. Charton, "Uranium (VI) on-chip microliter concentration measurements in a highly extended UV–visible absorbance linearity range," *Anal Chem*, vol. 90, no. 4, pp. 2456–2460, 2018.

[42] S. Wang, X. Huang, and C. Yang, "Mixing enhancement for high viscous fluids in a microfluidic chamber," *Lab Chip*, vol. 11, no. 12, pp. 2081–2087, 2011.

[43] A. Bordbar, S. Kheirandish, A. Taassob, R. Kamali, and A. Ebrahimi, "High-viscosity liquid mixing in a slug-flow micromixer: a numerical study," *J Flow Chem*, vol. 10, pp. 449–459, 2020.

[44] G. Cai, L. Xue, H. Zhang, and J. Lin, "A review on micromixers," *Micromachines (Basel)*, vol. 8, no. 9, p. 274, 2017.

[45] K. W. Oh, K. Lee, B. Ahn, and E. P. Furlani, "Design of pressure-driven microfluidic networks using electric circuit analogy," *Lab Chip*, vol. 12, no. 3, pp. 515–545, 2012.

[46] A. A. Deshmukh, D. Liepmann, and A. P. Pisano, "Continuous micromixer with pulsatile micropumps," in *Technical Digest of the IEEE Solid State Sensor and Actuator Workshop (Hilton Head Island, SC)*, Citeseer, 2000.

[47] Z. Yang, S. Matsumoto, H. Goto, M. Matsumoto, and R. Maeda, "Ultrasonic micromixer for microfluidic systems," *Sens Actuators A Phys*, vol. 93, no. 3, pp. 266–272, 2001.

[48] J. Yang *et al.*, "High sensitivity PCR assay in plastic micro reactors," *Lab Chip*, vol. 2, no. 4, pp. 179–187, 2002.

[49] C. Kumar *et al.*, "Modeling of mass transfer enhancement in a magnetofluidic micromixer," *Physics of Fluids*, vol. 31, no. 6, 2019.

[50] J. Zhang, G. He, and F. Liu, "Electro-osmotic flow and mixing in heterogeneous microchannels," *Phys Rev E*, vol. 73, no. 5, p. 56305, 2006.

[51] K.-R. Huang, J.-S. Chang, S. D. Chao, T.-S. Wung, and K.-C. Wu, "Study of active micromixer driven by electrothermal force," *Jpn J Appl Phys*, vol. 51, no. 4R, p. 47002, 2012.

[52] C. Huang and C. Tsou, "The implementation of a thermal bubble actuated microfluidic chip with microvalve, micropump and micromixer," *Sens Actuators A Phys*, vol. 210, pp. 147–156, 2014.

[53] P. Tabeling, M. Chabert, A. Dodge, C. Jullien, and F. Okkels, "Chaotic mixing in cross-channel micromixers," *Philosophical Transactions of the Royal Society of London. Series A: Mathematical, Physical and Engineering Sciences*, vol. 362, no. 1818, pp. 987–1000, 2004.

[54] Q. Xia and S. Zhong, "Quantification of liquid mixing enhanced by alternatively pulsed injection in a confined jet configuration," *J Vis (Tokyo)*, vol. 15, pp. 57–66, 2012.

[55] C. A. Cortes-Quiroz, A. Azarbadegan, I. D. Johnston, and M. C. Tracey, "Analysis and design optimization of an integrated micropump-micromixer operated for bio-MEMS applications," 2014.

[56] A. Hashmi, G. Yu, M. Reilly-Collette, G. Heiman, and J. Xu, "Oscillating bubbles: a versatile tool for lab on a chip applications," *Lab Chip*, vol. 12, no. 21, pp. 4216–4227, 2012.

[57] M. A. Deif, M. A. A. Eldosoky, H. W. Gomma, A. M. El-Garhy, and A. S. Ell-Azab, "Adaptive neuro-fuzzy inference system controller technique for lower urinary tract system disorders," *J Clin Eng*, vol. 40, no. 3, pp. 135–143, 2015.

[58] D. Ahmed, X. Mao, J. Shi, B. K. Juluri, and T. J. Huang, "A millisecond micromixer via single-bubble-based acoustic streaming," *Lab Chip*, vol. 9, no. 18, pp. 2738–2741, 2009.

[59] Q. Cao, X. Han, and L. Li, "An active microfluidic mixer utilizing a hybrid gradient magnetic field," *International Journal of Applied Electromagnetics and Mechanics*, vol. 47, no. 3, pp. 583–592, 2015.

[60] M. Hejazian, D.-T. Phan, and N.-T. Nguyen, "Mass transport improvement in microscale using diluted ferrofluid and a non-uniform magnetic field," *RSC Adv*, vol. 6, no. 67, pp. 62439–62444, 2016.

[61] A. Shamloo, M. Madadelahi, and A. Akbari, "Numerical simulation of centrifugal serpentine micromixers and analyzing mixing quality parameters," *Chemical Engineering and Processing: Process Intensification*, vol. 104, pp. 243–252, 2016.

[62] S. Haeberle, T. Brenner, H. Schlosser, R. Zengerle, and J. Ducrée, "Centrifugal micromixery," *Chemical Engineering & Technology: Industrial Chemistry-Plant Equipment-Process Engineering-Biotechnology*, vol. 28, no. 5, pp. 613–616, 2005.

[63] W. W.-F. Leung and Y. Ren, "Crossflow and mixing in obstructed and width-constricted rotating radial microchannel," *Int J Heat Mass Transf*, vol. 64, pp. 457–467, 2013.

[64] A. D. Stroock, S. K. W. Dertinger, A. Ajdari, I. Mezic, H. A. Stone, and G. M. Whitesides, "Chaotic mixer for microchannels," *Science (1979)*, vol. 295, no. 5555, pp. 647–651, 2002.

[65] P. B. Howell Jr *et al.*, "A microfluidic mixer with grooves placed on the top and bottom of the channel," *Lab Chip*, vol. 5, no. 5, pp. 524–530, 2005.

[66] S. Hossain and K.-Y. Kim, "Mixing analysis of passive micromixer with unbalanced three-split rhombic sub-channels," *Micromachines (Basel)*, vol. 5, no. 4, pp. 913–928, 2014.

[67] A. A. S. Bhagat, E. T. K. Peterson, and I. Papautsky, "A passive planar micromixer with obstructions for mixing at low Reynolds numbers," *Journal of micromechanics and microengineering*, vol. 17, no. 5, p. 1017, 2007.

[68] F. Schönfeld and S. Hardt, "Simulation of helical flows in microchannels," *AIChE Journal*, vol. 50, no. 4, pp. 771–778, 2004.

[69] T. S. Sheu, S. J. Chen, and J. J. Chen, "Mixing of a split and recombine micromixer with tapered curved microchannels," *Chem Eng Sci*, vol. 71, pp. 321–332, 2012.

[70] J. Branebjerg, P. Gravesen, J. P. Krog, and C. R. Nielsen, "Fast mixing by lamination," in *Proceedings of ninth international workshop on micro electromechanical systems*, IEEE, 1996, pp. 441–446.

[71] W. Buchegger, C. Wagner, B. Lendl, M. Kraft, and M. J. Vellekoop, "A highly uniform lamination micromixer with wedge shaped inlet channels for time resolved infrared spectroscopy," *Microfluid Nanofluidics*, vol. 10, pp. 889–897, 2011.

[72] H. Le The, H. Le-Thanh, N. Tran-Minh, and F. Karlsen, "A novel passive micromixer with trapezoidal blades for high mixing efficiency at low Reynolds number flow," in *2nd Middle East Conference on Biomedical Engineering*, IEEE, 2014, pp. 25–28.

[73] J. Yang, L. Qi, Y. Chen, and H. Ma, "Design and fabrication of a three dimensional spiral micromixer," *Chin J Chem*, vol. 31, no. 2, pp. 209–214, 2013.

[74] X. Li, H. Chang, X. Liu, F. Ye, and W. Yuan, "A 3-D overbridge-shaped micromixer for fast mixing over a wide range of reynolds numbers," *Journal of Microelectromechanical Systems*, vol. 24, no. 5, pp. 1391–1399, 2015.

[75] A.-S. Yang *et al.*, "A high-performance micromixer using three-dimensional Tesla structures for bio-applications," *Chemical Engineering Journal*, vol. 263, pp. 444–451, 2015.